Supporting Information

From a Piano-Stool to a Sandwich: A Stepwise Route for Improving the Slow Magnetic Relaxation Properties of Thulium

Katie L. M. Harriman,[a] *Ilia Korobkov,*[a] *and Muralee Murugesu**[a]

[a] Department of Chemistry and Biomolecular Sciences, University of Ottawa, Ottawa, Ontario K1N 6N5, Canada.

*Corresponding Author: M. Murugesu (E-mail: m.murugesu@uottawa.ca; Tel: +1 (613) 562 5800 ext 2733)

Contents

General Procedures and Starting Materials. All reactions and subsequent manipulations were performed under anaerobic and anhydrous conditions using a standard Schlenk-line or nitrogen-atmosphere glovebox. Tetrahydrofuran (THF) and dimethoxyethane (DME), were dried on columns of activated alumina using a J.C. Mayer solvent purification system, and degassed with successive freeze-pump-thaw cycles. All solvents were of least reagent grade and were stored over 3Å molecular sieves. Anhydrous TmI_2 and potassium metal were purchased from Sigma Aldrich; these chemicals were used as received. 18-crown-6 (18-c-6) was purchased from Sigma Aldrich and purified *via* vacuum sublimation at 0.019 Torr. 1,3,5,7-cyclooctatetraene was purchased from TCI and bubble degassed with argon prior to use. **K_2COT** was prepared as previously reported,[1] with the only modification occurring for the solvent, where THF was replaced with DME. The preparation of $[Tm(COT)I(THF)_2]$,[2] was modified from previously published reports as described below. Infrared spectra were recorded on a Nicolet Nexus 550 FT-IR spectrometer using transmission mode in the 4000-600 cm^{-1} range; solid samples were prepared under an inert atmosphere and sandwiched between transparent NaCl plates. NMR spectra were acquired on a Bruker Avance-II 300 MHz spectrometer at 298 K. Elemental analysis were conducted by Canadian Microanalytical, Delta, BC.

Preparation of $[Tm(COT)I(THF)_2]$ (1-Tm). Under an inert atmosphere, a solution of 1,3,5,7-cyclooctatetraene (0.1 mL, 0.888 mmol) in THF was added slowly to a slurry of TmI_2 (368 mg, 0.870 mmol) in THF. The green slurry became red upon immediate addition of 1,3,5,7-cyclooctatetraene. The solution was stirred for 30 min at room temperature and then filtered over a fine frit to remove any remaining TmI_2 and TmI_3. The filtrate was collected and concentrated, additional TmI_3 was precipitated. TmI_3 was removed *via* filtration over Celite, red block x-ray quality single crystals were grown from the filtrate at room temperature overnight. Isolated crystals are air and moisture sensitive. Yield = 72-74%. IR (neat, cm^{-1}): 2972 (br), 2892 (m), 1866 (m), 1754 (m), 1621 (m), 1563 (w), 1482 (w), 1470 (w), 1445 (w), 1366 (w), 1344 (m), 1311 (m), 1245 (m), 1182 (m), 1068 (m), 1018 (m), 853 (m), 799 (m), 750 (m), 717 (m), 671 (m), 627 (m). ^{1}H NMR (THF-d^8, 298 K, δ/ppm): 2.54 (s, 8 H, *THF*, FWHM: 92 Hz), 1.15 (s, 8 H, *THF*, FWHM: 138 Hz), -182.32 (br, s, 8 H, C_8H_8, FWHM: 4044 Hz). CHN analysis (found, calc.) for $C_{16}H_{24}IO_2Tm$: C (34.40, 35.31); H (4.60, 4.45); N (<0.3, 0.00).

Preparation of [K(18-c-6)(THF)$_2$][Tm(COT)$_2$] (2-Tm). Under an inert atmosphere, a solution of **K_2COT** (27 mg, 0.07 mmol) in THF is added dropwise to a solution of **1-Tm** (33 mg, 0.06 mmol) in THF at -35°C. The solution is stirred at room temperature for 20 min and the reaction mixture filtered over Celite and subsequently washed three times with THF. The filtrate was collected and concentrated. 1 equivalent of 18-crown-6 (16mg, 0.06 mmol) was added in 1 mL of THF. Single-crystal x-ray quality red needles were obtained after 48 h at room temperature. Isolated crystals are air and moisture sensitive. Yield = 66%. IR (neat, cm^{-1}): 2852 (w), 1599 (w), 1469 (m), 1349 (m), 1282 (m), 1246 (m), 1234 (m), 1104 (m), 964 (s), 897 (s), 838 (s), 800 (m), 760 (m), 743 (s), 681 (s), 628 (w). ^{1}H NMR (THF-d^8, 298 K, δ/ppm): 78.22 (br, s, 24 H, *18C6*, FWHM: 1075 Hz), 5.40 (br, s, 8 H, *THF*, FWHM: 388 Hz), 0.07 (br, s, 8 H, *THF*, FWHM: 308 Hz), -177.72 (br, s, 16 H, C_8H_8, FWHM: 9554 Hz). CHN analysis (found, calc.) for $C_{36}H_{56}KO_8Tm$: C (52.09, 52.42); H (6.17, 6.84); N (<0.3, 0.00).

Single Crystal X-ray Diffraction Studies. Structural information has been previously reported for **1-Tm**. However; for the purposes of completeness our parameters are included below. Data collection results for compounds **1-Tm** and **2-Tm** represent the best data sets obtained in several trials for each sample. The crystals were mounted on thin glass fibers using paraffin oil. Prior to data collection crystals were cooled to 200.15 K. Data were collected on a Bruker AXS KAPPA or SMART single crystal diffractometer equipped with a sealed Mo tube source (wavelength 0.71073 Å) APEX II CCD detector. Raw data collection and processing were performed with APEX II software package from BRUKER AXS.[3] Initial unit cell parameters were determined from 60 data frames with 0.3° ω scan each, collected at the different sections of the Ewald sphere. Semi-empirical absorption corrections based on equivalent reflections were applied.[4] Systematic absences in the diffraction data-set and unit-cell parameters were consistent with monoclinic **P***2$_1$/n* (№14) for compound **1-Tm** and triclinic **P**-*1* (№2) for compound **2-Tm**. Solutions in the centrosymmetric space groups for both samples yielded chemically reasonable and computationally stable results of refinement. Structures were solved by direct methods, completed with difference Fourier synthesis, and refined with full-matrix least-squares procedures based on F^2.

For all the compounds all hydrogen atoms positions were calculated based on the geometry of related non-hydrogen atoms. All hydrogen atoms were treated as idealized

contributions during the refinement. All scattering factors are contained in several versions of the SHELXTL program library, with the latest version used being v.7.14.[5] Crystallographic data and selected data collection parameters are reported in Table S1.

Table S1. Crystallographic data and selected data collection parameters.

Compound	**1-Tm**	**2-Tm**
Empirical formula	$C_{16}H_{24}IO_2Tm$	$C_{36}H_{56}KO_8Tm$
Formula weight	544.18	824.83
Crystal size, mm	0.130x0.080x0.060	0.300x0.100x0.070
Crystal system	Monoclinic	Triclinic
Space group	**P***2₁/n*	**P**-*1*
Z	4	1
a, Å	8.4178(2)	7.7365(2)
b, Å	9.3602(3)	9.3103(2)
c, Å	22.0805(6)	13.1135(3)
α, °	90	85.0171(12)
β, °	97.3536(14)	83.5823(11)
γ, °	90	89.4078(13)
Volume, $Å^3$	1725.46(8)	935.09(4)
Calculated density, Mg/m^3	2.095	1.465
Absorption coefficient, mm^{-1}	3.930	2.530
T (K)	200(2)	200(2)
F(000)	1032	424
Θ range for data collection, °	2.366 to 28.317	2.196 to 28.320
Limiting indices	h = ±11, k = ±112, l = ±29	h = ±10, k = ±12, l = ±17
Reflections collected / unique	14763	8104
R(int)	0.0219	0.0130
Completeness to Θ = 28.32, %	98.7	97.7
Max. and min. transmission	0.7457 and 0.4954	0.7457 and 0.5254
Data / restraints / parameters	4228 / 96 / 199	4519 / 6 / 220
Goodness-of-fit on F^2	1.046	1.033
Final R indices [I>2σ(I)][a]	R1 = 0.0341, wR2 = 0.0743	R1 = 0.0198, wR2 = 0.0525
R indices (all data)	R1 = 0.0420, wR2 = 0.0780	R1 = 0.0199, wR2 = 0.0525
Largest diff. peak/hole, $e \cdot Å^{-3}$	2.897 and -2.889	0.792 and -0.519

[a] $R = R_1 = \sum||F_0| - |F_c|| / \sum|F_0|$; $wR_2 = \{\sum[w (F_0^2 - F_c^2)^2 / \sum[w(F_0)^2]]\}^{1/2}$; $w = 1/[\delta^2(F_o^2) + (ap)^2 + bp]$, where $p = [\max (F_0^2, 0) + 2F_c^2]/3$

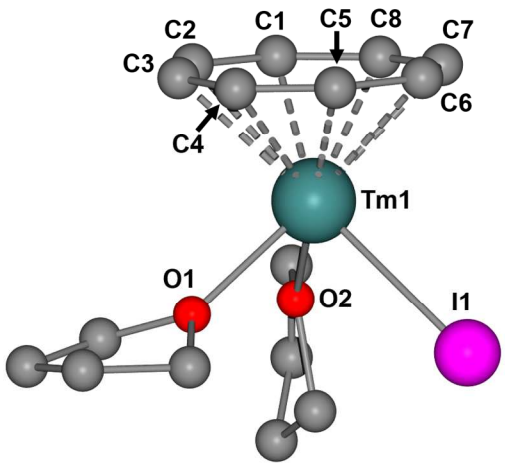

Figure S1. X-ray crystal structure of [Tm(COT)I(THF)$_2$] (**1-Tm**). Hydrogen atoms and disorder have been omitted for clarity. Selected bond distances (Å) and angles (deg) follow: Tm1-O1, 2.337(4); Tm1-O2, 2.353(4); Tm1-C1, 2.534(6), Tm1-C2, 2.555(7); Tm1-C3, 2.533(7), Tm1-C4, 2.525(7); Tm1-C5, 2.515(7); Tm1-C6, 2.524(6); Tm1-C7, 2.515(5); Tm1-C8, 2.516(5), Tm1-I1, 3.0245(5); O1-Tm1-O2, 78.72(15); O1-Tm1-I1, 87.50(12); O2-Tm1-I1, 85.76(12).

Table S2. Tm-C_{COT} bond distances obtained from single crystal X-ray diffraction studies

Bond	**1-Tm**	**2-Tm**
Tm1-C1 (Å)	2.534(6)	2.615(2)
Tm1-C2 (Å)	2.555(7)	2.598(2)
Tm1-C3 (Å)	2.533(7)	2.598(2)
Tm1-C4 (Å)	2.525(7)	2.617(2)
Tm1-C5 (Å)	2.515(7)	2.620(2)
Tm1-C6 (Å)	2.524(6)	2.600(2)
Tm1-C7 (Å)	2.515(5)	2.598(2)
Tm1-C8 (Å)	2.516(5)	2.604(2)

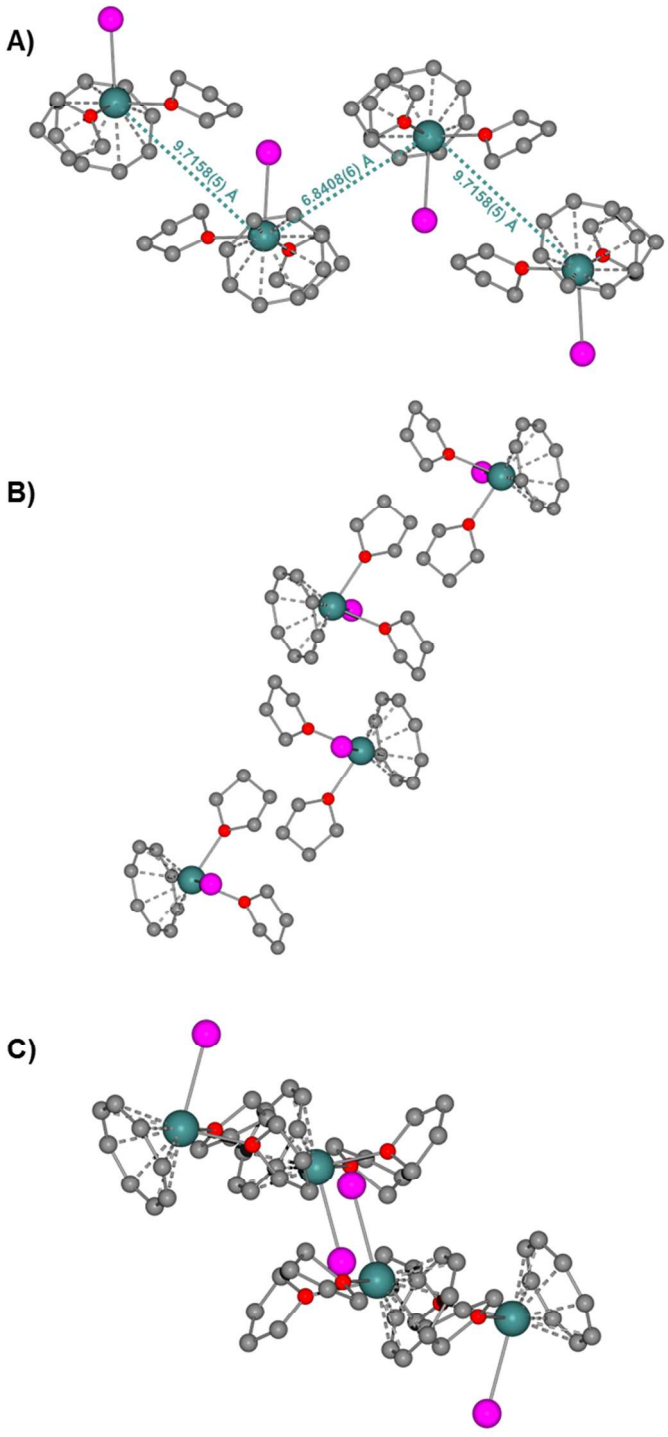

Figure S2. Crystallographic packing arrangements of **1-Tm**: (a) along the *a*-axis, (b) along the *b*-axis, and (c) along the *c*-axis. Closest intermolecular Tm---Tm distances shown in (a). Color code: Tm; teal, I; pink, O; red, C; grey. Hydrogen atoms and disorder have been omitted for clarity.

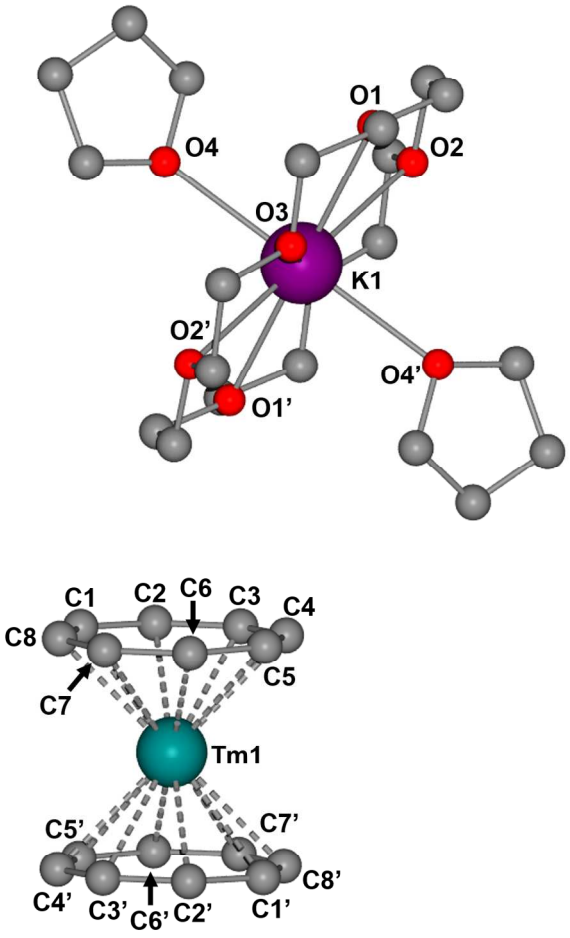

Figure S3. X-ray crystal structure of $[K(18\text{-crown-6})(THF)_2][Tm(COT)_2]$ (**2-Tm**). Hydrogen atoms and disorder have been omitted for clarity. Selected bond distances (Å) follow: Tm1-C1, 2.615(2); Tm1-C2, 2.598(2); Tm1-C3, 2.598(2); Tm1-C4, 2.617(2); Tm1-C5, 2.620(2); Tm1-C6, 2.600(2); Tm1-C7, 2.598(2); Tm1-C8, 2.604(2).

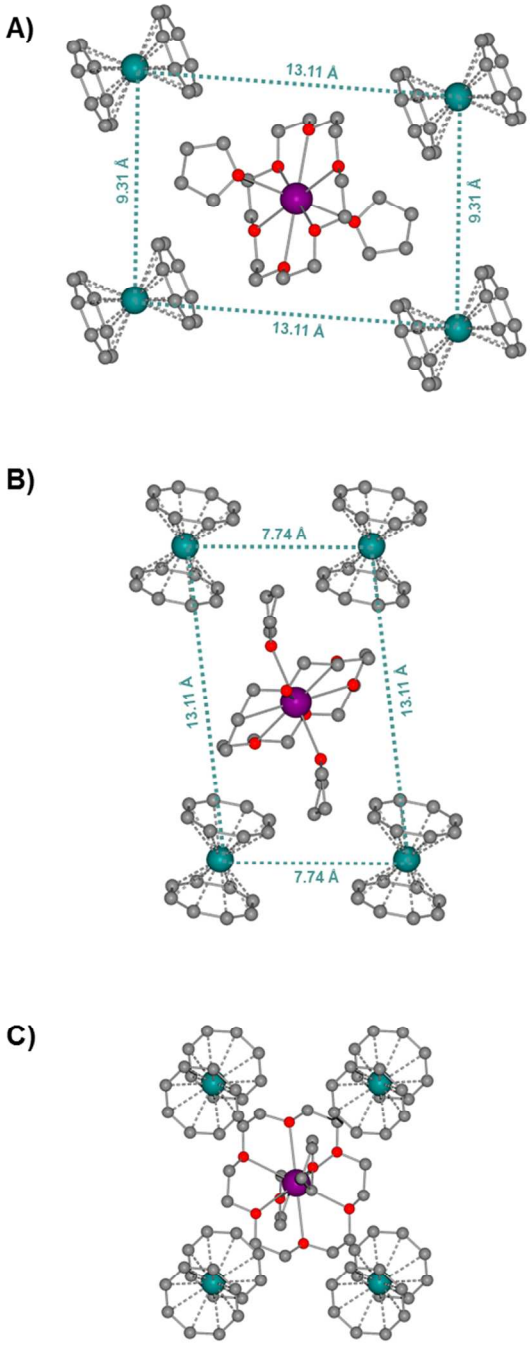

Figure S4. Crystallographic packing arrangements of **2-Tm**: (a) along the *a*-axis, (b) along the *b*-axis, and (c) along the *c*-axis. Closest intermolecular Tm---Tm distances shown in (a) and (b). Color code: Tm; teal, O; red, C; grey. Hydrogen atoms and disorder have been omitted for clarity.

Magnetic Measurements. The magnetic susceptibility measurements were obtained using a Quantum Design SQUID magnetometer MPMS-XL7 operating between 1.8 and 300 K. DC measurements were performed on polycrystalline samples of 12 mg for **1-Tm** and **2-Tm**. The samples were wrapped in a polyethylene bag under an inert atmosphere, and subjected to a field of 0 to 7 T. The magnetization data were collected at 100 K to check for ferromagnetic impurities that were absent in both samples. Diamagnetic corrections were applied for the sample holder and the inherent diamagnetism of the sample was estimated with the use of Pascals constants.

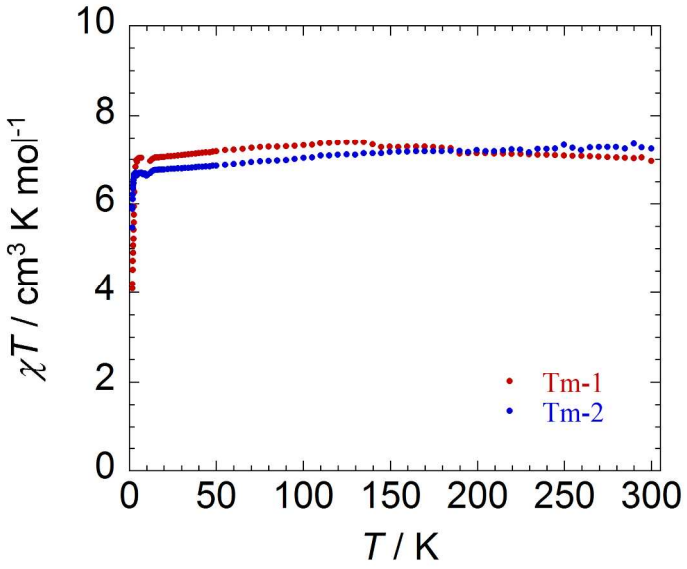

Figure S5. Temperature dependence of the χT product under 1000 Oe for **1-Tm** (red) and **2-Tm** (blue), where χ is the molar magnetic susceptibility as defined by *M/H*. Room temperature values of 6.96 and 7.24 cm^3Kmol^{-1} are obtained for **1-Tm** and **2-Tm** respectively.

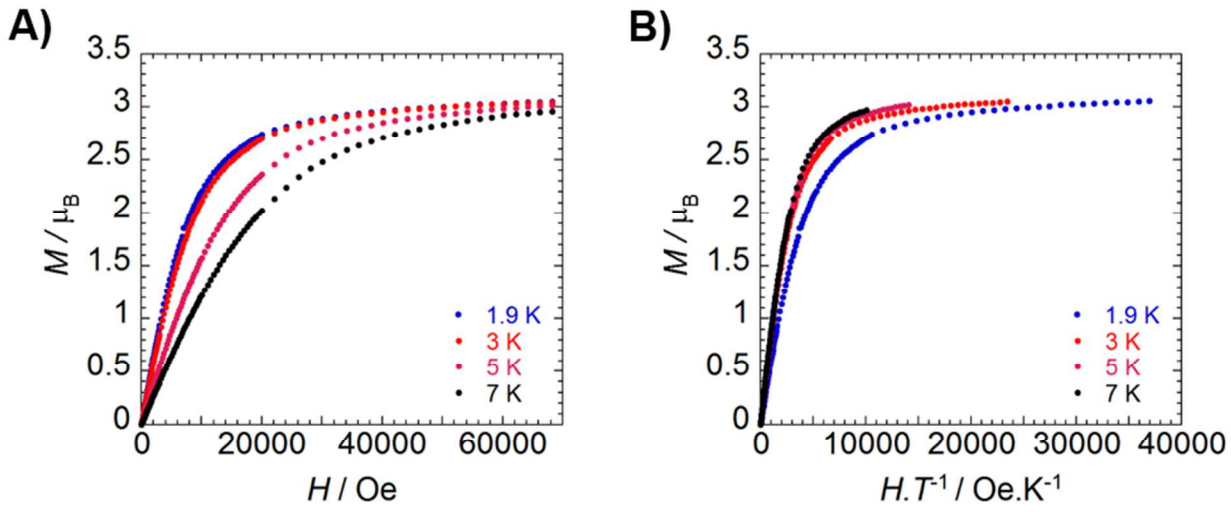

Figure S6. Solid state field dependence of A) the magnetization and B) the reduced magnetization for **1-Tm** at the indicated temperatures.

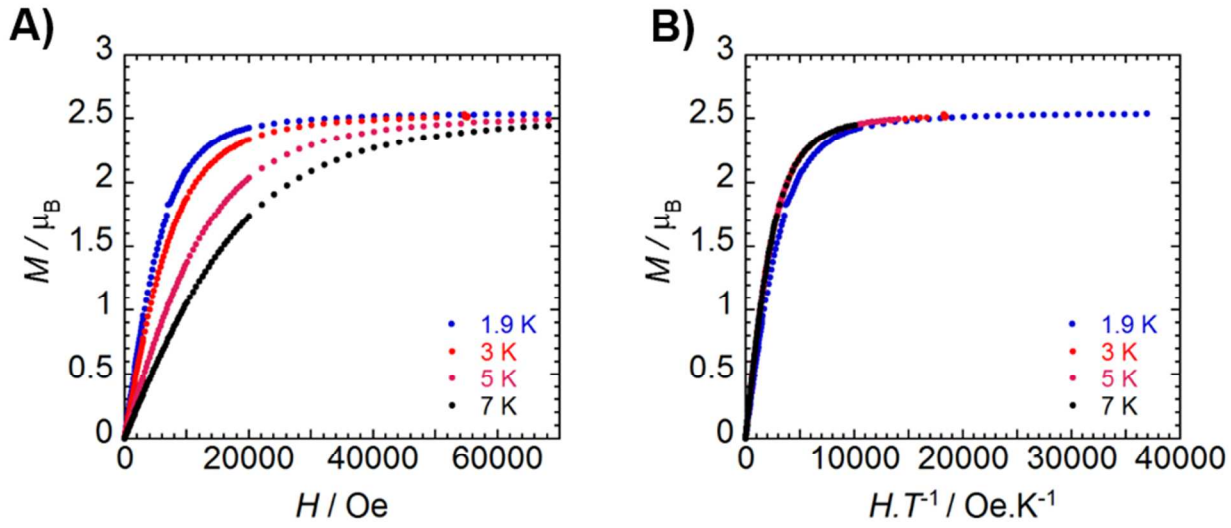

Figure S7. Solid state field dependence of A) the magnetization and B) the reduced magnetization for **2-Tm** at the indicated temperatures.

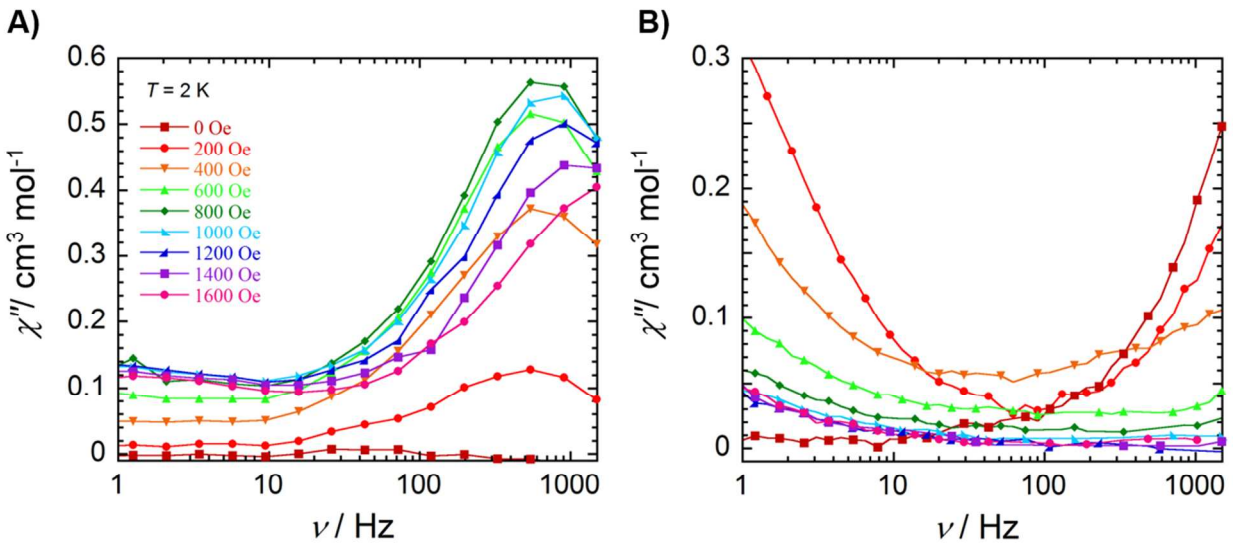

Figure S8. Frequency dependence of the out-of-phase (χ") magnetic susceptibility for (a) **1-Tm** and (b) **2-Tm**. Data collected at 2 K as a function of applied static field (0-1600 Oe). Solid lines are guides for the eye.

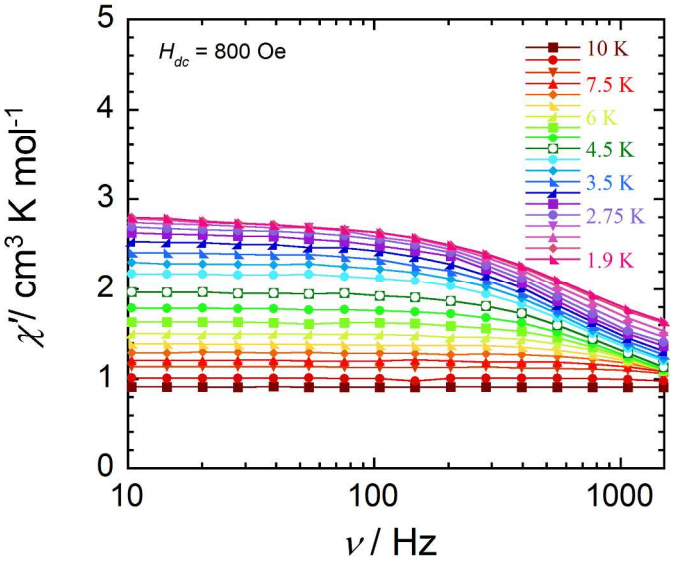

Figure S9. Frequency dependence of the in phase (χ') magnetic susceptibility for **1-Tm**. Data collected under an applied static field of 800 Oe as a function of temperature (1.9-10 K). Solid lines are guides for the eye.

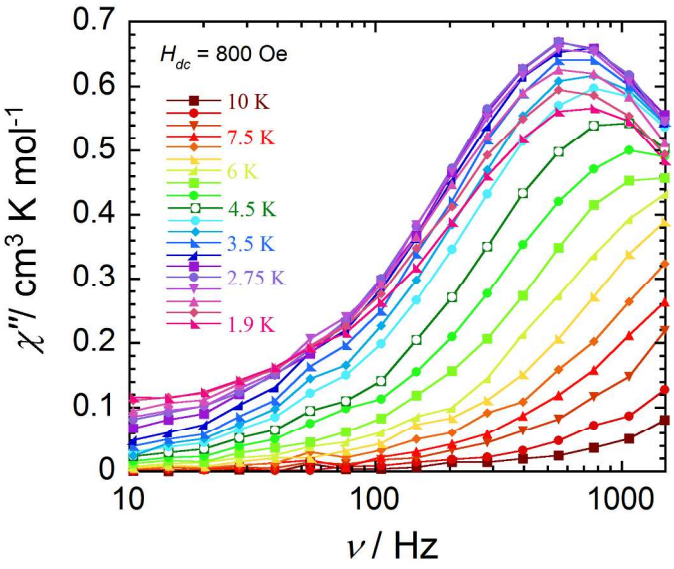

Figure S10. Frequency dependence of the out-of-phase (χ") magnetic susceptibility for **1-Tm**. Data collected under an applied static field of 800 Oe as a function of temperature (1.9-10 K). Solid lines are guides for the eye.

Table S3. Fitting of the in phase (χ') magnetic susceptibility plot to the generalized Debye model. Best fit parameters yield values of τ, α, χ_S, and χ_T for **1-Tm** under 800 Oe dc field at varying temperatures.

T (K)	τ (s)	α	χ_S	χ_T	χ_T- χ_S	ν (Hz)
1.9	1.64095E-4	0.27907	0.84476	2.83421	1.98945	1175.50162
2	2.00636E-4	0.24302	1.001	2.82394	1.82294	881.78594
2.25	2.08234E-4	0.22128	0.92316	2.81233	1.88917	838.08232
2.5	2.52842E-4	0.16424	1.04228	2.75937	1.71709	649.28528
2.75	2.66683E-4	0.12997	1.05094	2.69691	1.64597	605.54175
3	2.51401E-4	0.14998	0.95319	2.64585	1.69266	652.48988
3.25	2.50217E-4	0.12818	0.94603	2.54277	1.59673	652.132
3.5	2.46567E-4	0.10338	0.94991	2.42438	1.47447	659.56301
3.75	2.36087E-4	0.07901	0.9301	2.3013	1.3712	684.41756
4	2.19653E-4	0.08397	0.88899	2.18995	1.30096	740.62901
4.5	1.71163E-4	0.08535	0.73604	1.97424	1.2382	970.41159
5	1.49593E-4	0.07376	0.71667	1.79421	1.07754	1106.13432
5.5	1.20216E-4	0.06341	0.65858	1.63727	0.9787	1410.24444

Table S4. Fitting of the out-of-phase (χ") magnetic susceptibility plot to the generalized Debye model. Best fit parameters yield values of τ, α, χ_S, and χ_T for **1-Tm** under 800 Oe dc field at varying temperatures. Below 2.25 K a reasonable fit could not be obtained.

T (K)	τ (s)	α	χ_S	χ_T	χ_T- χ_S	ν (Hz)
1.9	-	-	-	-	-	-
2	-	-	-	-	-	-
2.25	-	-	-	-	-	-
2.5	2.07099E-4	0.27379	0.19088	2.16588	1.975	615.67206
2.75	2.32678E-4	0.21168	0.01219	1.84431	1.83213	593.52779
3	2.36909E-4	0.17868	0.03365	1.7879	1.75424	605.25179
3.25	2.38612E-4	0.14819	0.00325	1.66843	1.66518	740.22646
3.5	2.30313E-4	0.12092	0.01039	1.57751	1.56712	747.92297
3.75	2.12287E-4	0.11124	0.02836	1.51749	1.48913	784.75762
4	1.95983E-4	0.10328	0.11953	1.53802	1.41849	820.5322
4.5	1.73475E-4	0.07434	0.00858	1.24256	1.23398	892.68053
5	1.39793E-4	0.08302	0.00838	1.1546	1.14622	1162.98578
5.5	1.2359E-4	0.03711	0.02052	1.00004	0.97952	1245.89192

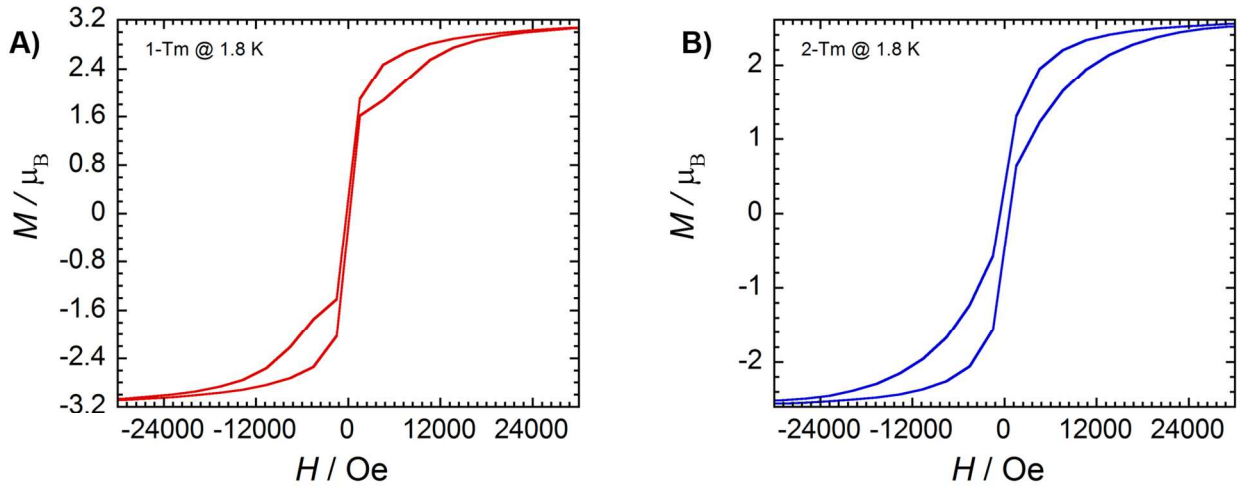

Figure S11. Magnetic hysteresis data for (a) **1-Tm** and (b) **2-Tm** collected at 1.8 K and an average sweep rate of 23 Oe s^{-1}. In all measurements, data were collected starting at H = 0 Oe, sweeping to H = 50 kOe and then cycling to H = -50 kOe and back to H = 50 kOe.

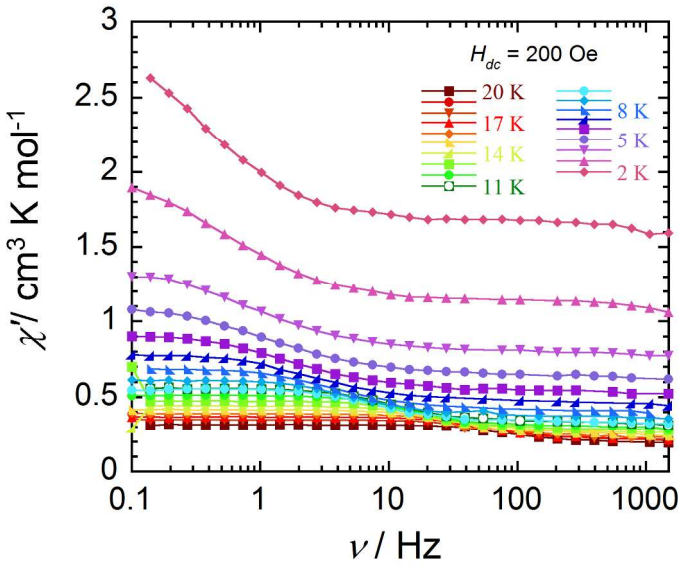

Figure S12. Frequency dependence of the in phase (χ') magnetic susceptibility for **2-Tm**. Data collected under an applied static field of 200 Oe as a function of temperature (2-20 K). Solid lines are guides for the eye.

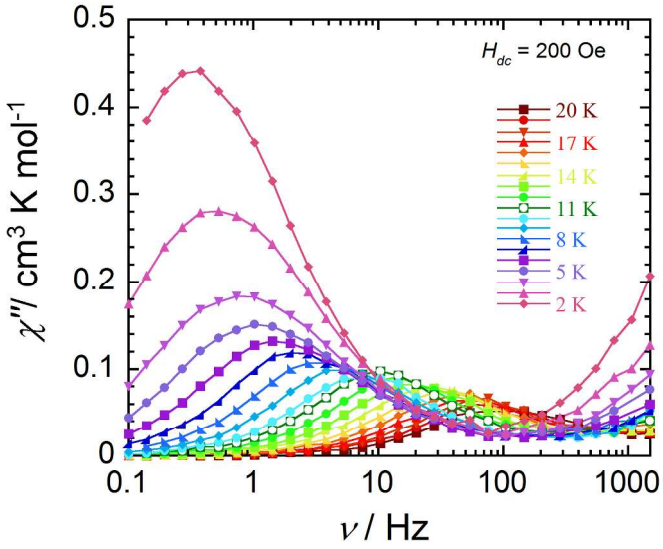

Figure S13. Frequency dependence of the out-of-phase (χ") magnetic susceptibility for **2-Tm**. Data collected under an applied static field of 200 Oe as a function of temperature (2-20 K). Solid lines are guides for the eye.

Table S5. Fitting of the in phase (χ') magnetic susceptibility plot to the generalized Debye model. Best fit parameters yield values of τ, α, χ_S, and χ_T for **2-Tm** under 200 Oe dc field at varying temperatures.

T (K)	τ (s)	α	χ_S	χ_T	χ_T- χ_S	ν (Hz)
2	0.53783	0.29655	1.6471	3.11425	0.36451	0.24733
2.5	0.41284	0.31012	1.33623	2.50744	0.33708	0.36006
3	0.33061	0.32484	1.11383	2.09476	0.308	0.45748
3.5	0.29039	0.34894	0.9587	1.81733	0.28869	0.52106
4	0.18935	0.31112	0.78944	1.39708	0.26388	0.83586
4.5	0.16712	0.32317	0.70138	1.2587	0.2496	0.94793
5	0.14097	0.31629	0.63577	1.13608	0.23581	1.1305
5.5	0.11008	0.28573	0.58242	1.02212	0.22099	1.46047
6	0.08978	0.26463	0.53635	0.93427	0.23343	1.79457
6.5	0.07304	0.25529	0.49762	0.86213	0.21171	2.20983
7	0.0584	0.24637	0.46245	0.79953	0.18259	2.76544
7.5	0.04712	0.19086	0.43585	0.74385	0.17788	3.4218
8	0.03921	0.19559	0.41014	0.69882	0.16024	4.10618
8.5	0.03162	0.15918	0.39011	0.65399	0.16035	5.0693
9	0.0265	0.14431	0.36845	0.61805	0.15082	6.04655
9.5	0.02207	0.14783	0.3529	0.5887	0.13763	7.25451
10	0.01842	0.10728	0.33458	0.55557	101.17069	8.66246
11	0.01365	0.13571	0.32914	0.56258	0.11753	11.69769
12	0.0098	0.09398	0.30178	0.51349	0.36451	16.24152
13	0.00785	-4.69662E-22	0.29076	0.47335	0.33708	20.74943
14	0.00563	0.09822	0.26651	0.44439	0.308	28.26009
15	0.00479	-6.93947E-19	0.25479	0.41503	0.28869	33.94795
16	0.0038	0.10109	0.23274	0.39309	0.26388	41.94954
17	0.00273	0.06416	0.21932	0.37014	0.2496	58.288
18	0.0023	0.04769	0.21315	0.35077	0.23581	69.07968
19	0.00182	0.04284	164.77257	265.94326	0.22099	87.54812
20	0.00189	-5.7709E-19	0.19957	0.3171	0.23343	87.5531

Table S6. Fitting of the out-of-phase (χ") magnetic susceptibility plot to the generalized Debye model. Best fit parameters yield values of τ, α, χ_S, and χ_T for **2-Tm** under 200 Oe dc field at varying temperatures.

T (K)	τ (s)	α	χ_S	χ_T	χ_T- χ_S	ν (Hz)
2	0.53097	0.31762	1.11874	2.58624	1.46751	0.36419
2.5	0.38121	0.32046	1.427	2.57543	1.14844	0.40337
3	0.3037	0.33868	1.34605	2.3071	0.96105	0.427
3.5	0.24809	0.32897	1.5	2.30377	0.80377	0.70548
4	0.18251	0.34637	0.45536	1.07963	0.62427	0.76693
4.5	0.14972	0.35073	0.59411	1.15128	0.55717	1.01907
5	0.12296	0.31137	0.67274	1.15301	0.48027	1.08959
5.5	0.10209	0.27502	0.63922	1.06349	0.42427	1.15502
6	0.08453	0.24996	0.61716	1.00053	0.38337	1.49205
6.5	0.06821	0.24094	0.79991	1.15474	0.35483	1.6296
7	0.05759	0.21298	0.67593	1.00041	0.32448	2.14474
7.5	0.04655	0.20381	0.57332	0.87708	0.30376	2.90186
8	0.0388	0.19911	0.79631	1.08342	0.28711	3.07979
8.5	0.03188	0.18419	0.75969	1.02661	0.26692	4.18704
9	0.02602	0.18383	0.82003	1.07595	0.25592	4.5285
9.5	0.0209	0.19595	0.81742	1.06284	0.24542	6.20014
10	0.01691	0.21376	0.80503	1.04572	0.24069	7.67547
11	0.01272	0.19113	0.82247	1.06895	0.24648	9.15293
12	0.01272	0.19113	0.82247	1.06895	0.24648	14.59264
13	0.00662	0.12294	0.83179	1.03162	0.19983	20.16619
14	0.00529	0.12595	0.81643	1.00851	0.19209	23.96638
15	0.0035	0.21998	0.80204	1.00004	0.198	32.74497
16	0.00294	0.20968	0.82952	1.01173	0.18221	44.85124
17	0.00257	0.14696	0.84878	1.0086	0.15982	56.11982
18	0.00194	0.17408	0.84572	1.00872	0.16301	72.36432
19	0.00175	0.15885	0.85383	1.00341	0.14958	75.0363
20	0.00135	0.17588	0.862	1.00578	0.14377	81.48001

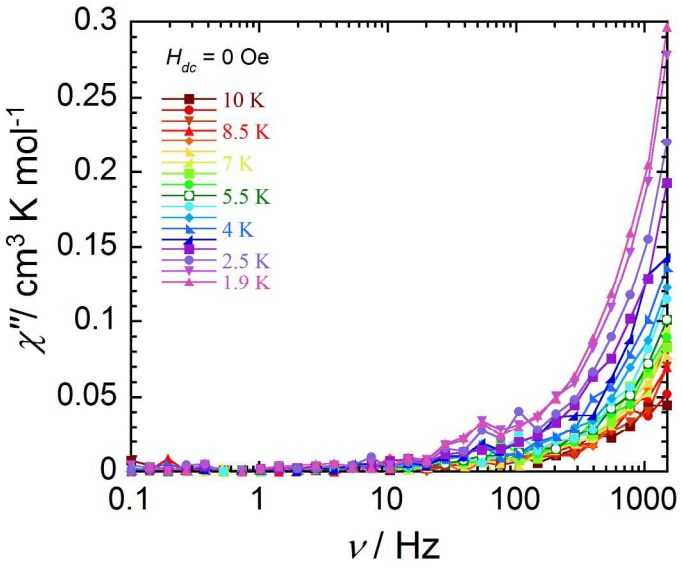

Figure S14. Frequency dependence of the out-of-phase (χ") magnetic susceptibility for **2-Tm**. Data collected under an applied static field of 0 Oe as a function of temperature (1.9-10 K). Solid lines are guides for the eye.

References

1. Meihaus, K. R.; Long, J. R., *J. Am. Chem. Soc.* **2013,** *135*, 17952-17957.
2. Fedushkin, I. L.; Bochkarev, M. N.; Dechert, S.; Schumann, H., *Chem. Eur. J.* **2001,** *7*, 3558-3563.
3. v.2012, A. S. S.; Bruker AXS: Madison, W., 2005.
4. Blessing, R. H., *Acta Crystallogr., Sect. A: Found. Crystallogr.* **1995,** *51*, 33-38.
5. Sheldrick, G. M., *Acta Crystallogr., Sect. A: Found. Crystallogr.* **2008,** *64*, 112-122.